Laminar Flow of a Heat-Generating Fluid in a Parallel-Plate Channel

E. M. SPARROW, J. L. NOVOTNY, and S. H. LIN

University of Minnesota, Minneapolis, Minnesota

The study of fluid flows with internal heat generation has been stimulated by modern applications such as the nuclear reactor. For laminar forced-convection flow in a circular tube analytical treatment of the heat-generating fluid has been carried out for the case of uniform tube wall temperature by Topper (*1*) and for prescribed wall heat flux by Sparrow and Siegel (*2*). These analyses provide results in the thermal entrance region of the tube as well as in the fully developed region. The predictions of reference 2 have recently been substantiated experimentally by Inman (*3*) in an apparatus consisting of an insulated tube through which was pumped an electrolyte. The heat generation was achieved by passing an electric current through the fluid. An analysis of the turbulent flow problem that corresponds to the laminar flow study of reference 2 has also been carried out (*4*).

In contrast to the rather complete investigation for the circular tube the forced-convection heat-generating flow in a parallel-plate channel has seen only limited study. This has been confined to consideration of the fully developed heat transfer for the uniform wall heat flux boundary condition (*5, 6*).

The present investigation aims to treat the heat-generating laminar flow in a parallel-plate channel in a very general way. An analysis including both prescribed wall temperature and prescribed wall heat flux is carried out for both the thermal entrance region and the fully developed region. Consideration is given not only to the basic cases of uniform wall temperature and uniform wall heat flux but also to arbitrary longitudinal distributions of the wall temperature or wall heat flux. The internal heat generation in the fluid may also have arbitrary longitudinal and transverse variations. In addition the analytical work just described will be compared with temperature measurements for flow of an electrolyte between parallel plates (*9*). It is thus seen that the present investigation covers approximately as much material for the parallel-plate channel as was contained in the three aforementioned references (*1, 2, 3*) for the circular tube, with the uniform wall temperature case actually receiving a somewhat more complete treatment here.

A schematic diagram of the system under consideration is presented in Figure 1. Fluid flows from left to right. The part of the channel to the left of $x = 0$ is a hydrodynamic starting section of sufficient length so that the flow arriving at $x = 0$ is fully developed. A heating process takes place in the section of the channel to the right of $x = 0$. This may include an internal heat generation in the fluid and a heat transfer at the wall under the condition of prescribed heat flux or prescribed surface temperature. The height of the channel is $2a$, and y is the cross-sectional coordinate measuring distances from the channel center line.

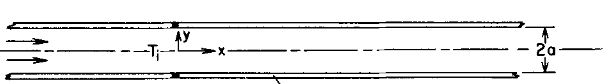

Fig. 1. Parallel plate channel.

This report will be subdivided into two major sections respectively dealing with internal heat generation in the presence of a prescribed wall temperature and with internal heat generation in the presence of a prescribed heat flux.

INTERNAL HEAT GENERATION WITH PRESCRIBED SURFACE TEMPERATURE

In the development which follows it will be convenient to begin with the case in which both the heat generation and the wall temperature are longitudinally uniform. This will facilitate later generalization to include nonuniform distributions of these quantities.

Uniform Heat Generation and Uniform Wall Temperature

Consideration is given to a fluid with a uniform temperature T_i entering a duct whose walls are held at a uniform temperature T_w. Additionally a uniform internal heat generation S (energy/time-volume) begins at $x = 0$. The energy transfer processes in the fluid are governed by the energy conservation principle

$$\rho c_p u \, \partial T/\partial x = k \, \partial^2 T/\partial y^2 + S \quad (1)$$

Equation (1) is written for constant fluid properties; longitudinal conduction is also neglected relative to transverse conduction.

The linearity of the energy equation suggests that the temperature $T(x, y)$ be written as a sum of two parts

$$T(x, y) = T_T(x, y) + T_{TS}(x, y) \quad (2a)$$

in which T_T corresponds to the problem in which a nongenerating fluid at T_i enters a duct whose wall temperature is T_w, and T_{TS} corresponds to the problem in which a heat generating fluid at $T = 0$ enters a duct whose wall temperature is also $T = 0$. It is convenient to rewrite Equation (2*a*) in the form

$$\frac{T(x, y) - T_w}{T_i - T_w} = \frac{T_T(x, y) - T_w}{T_i - T_w} + \frac{T_{TS}(x, y)}{T_i - T_w} = \theta_T + \theta_{TS} \quad (2b)$$

The governing equations for θ_T and θ_{TS} are

$$\frac{1}{4}\frac{u}{\bar{u}}\frac{\partial \theta_T}{\partial \xi} = \frac{\partial^2 \theta_T}{\partial \eta^2}, \quad \frac{1}{4}\frac{u}{\bar{u}}\frac{\partial \theta_{TS}}{\partial \xi} = \frac{\partial^2 \theta_{TS}}{\partial \eta^2} + \frac{S a^2}{k(T_i - T_w)} \quad (3)$$

The velocity distribution $u/\bar{u}$ appearing in Equation (3) is the well-known parabola

$$u/\bar{u} = (3/2)\,(1 - \eta^2) \quad (4)$$

When one takes cognizance of the foregoing physical interpretation of T_T and T_{TS}, the boundary conditions on θ_T and θ_{TS} can immediately be written:

$$\text{at } \eta = \pm 1, \quad \theta_T = 0 \quad \text{and } \theta_{TS} = 0 \quad (5a)$$

$$\text{at } \xi = 0, \quad \theta_T = 1 \quad \text{and } \theta_{TS} = 0 \quad (5b)$$

The problem of solving for θ_T and θ_{TS} is most conveniently attacked by the Graetz method. This approach is

TABLE 1. EIGENVALUES AND ASSOCIATED RESULTS,* PRESCRIBED WALL TEMPERATURE

n	β_n	$Y_n'(1)$	$C_{n,T}$	$C_{n,TS}$
1	1.6816	−1.4292	1.2008	−0.52047
2	5.6699	3.8071	−0.29916	0.025212
3	9.6682	−5.9202	0.16083	−0.0065735
4	13.6677	7.8925	−0.10744	0.0027491
5	17.6674	−9.7709	0.079646	−0.0014410
6	21.6672	11.5798	−0.062776	0.00086255
7	25.6671	−13.3339	0.051519	−0.00056346
8	29.6670	15.0430	−0.043511	0.00039161
9	33.6670	−16.7141	0.037542	−0.00028504
10	37.6669	18.3525	−0.032933	0.00021503

* $Y_n(0) = 1$ for all n.

standard in heat transfer analysis and need not be repeated here in detail. A general description may be found in the text by Jakob (*7*), and the aforementioned references (*1, 2,* and *4*) may serve as illustrative applications. The solution for θ_T is

$$\theta_T = \sum_{n=1}^{\infty} C_{n,T}\, Y_n(\eta)\, e^{-(8/3)\beta_n^2 \xi} \tag{6}$$

in which β_n^2 and Y_n are respectively the eigenvalues and eigenfunctions of the mathematical system

$$d^2Y_n/d\eta^2 + \beta_n^2(1-\eta^2)\, Y_n = 0; \qquad Y_n(1) = 0, \quad dY_n/d\eta(0) = 0 \tag{7}$$

The $C_{n,T}$ are determined so as to satisfy the condition that $\theta_T = 1$ at the entrance:

$$C_{n,T} = \left[\int_0^1 Y_n(1-\eta^2)\,d\eta\right] \Big/ \left[\int_0^1 Y_n^2(1-\eta^2)\,d\eta\right] \tag{7a}$$

Similarly the solution for θ_{TS} is

$$\theta_{TS} = \frac{S\,a^2}{k(T_i - T_w)}\left\{\frac{1}{2}(1-\eta^2) + \sum_{n=1}^{\infty} C_{n,TS}\, Y_n(\eta)\, e^{-(8/3)\beta_n^2\xi}\right\} \tag{8}$$

As in the foregoing the β_n^2 and Y_n are the eigenvalues and eigenfunctions of Equation (7), but now the $C_{n,TS}$ are

$$C_{n,TS} = -\left[\frac{1}{\beta_n^2}\int_0^1 Y_n\,d\eta\right] \Big/ \left[\int_0^1 Y_n^2\,(1-\eta^2)\,d\eta\right] \tag{8a}$$

in order to satisfy the condition $\theta_{TS} = 0$ at the entrance. By inspection of Equations (6) and (8) it is seen that there is a distinct difference in the solutions for θ_T and θ_{TS}; for large downstream distances $\theta_T \to 0$ ($T_T \to T_w$), while θ_{TS} approaches a parabolic form. The latter is the fully developed solution as given in references *5* and *6*.

To complete the solution it is necessary to find the eigenvalues and eigenfunctions of Equation (7) and to carry out the integrations for the C_n in equations (6*a*) and (8*a*). This has been done numerically, with a Control Data 1604 electronic digital computer. Information from these numerical solutions, selected to supplement the forthcoming heat transfer calculation, has been listed in Table 1. In this connection it may be mentioned that wherever comparison was possible there was excellent agreement with the listing of Brown (*8*) who calculated the first ten eigenfunctions of Equation (7).

The quantity which is perhaps of greatest practical interest is the heat flux q at the wall. By applying Fourier's Law $q = -k(\partial T/\partial y)_{y=a}$ to the foregoing temperature solution an expression for the local heat flux is obtained:

$$\frac{qa}{k(T_i - T_w)} = \left[-\Sigma\, C_{n,T}\, Y_n'(1)\, e^{-(8/3)\beta_n^2\xi}\right] + \frac{S\,a^2}{k(T_i - T_w)}\left[1 - \Sigma\, C_{n,TS}\, Y_n'(1)\, e^{-(8/3)\beta_n^2\xi}\right] \tag{9a}$$

$$= \left[\frac{q_T\, a}{k(T_i - T_w)}\right] + \frac{S\,a^2}{k(T_i - T_w)}\left[\frac{q_{TS}}{Sa}\right] \tag{9b}$$

The bracketed quantities of Equation (9*a*) have been given physical meaning in Equation (9*b*); q_T is the local heat flux to a duct wall at T_w from a nongenerating fluid which enters the duct at T_i, and q_{TS} is the local heat flux to a duct wall at $T = 0$ from a heat generating fluid which enters the duct at temperature $T = 0$. Clearly q_T and q_{TS} are completely independent of one another. Also the quantities $q_T a/k\ (T_i - T_w)$ and q_{TS}/Sa depend only upon the position coordinate ξ. Thus each one may be calculated once and for all and may be regarded as a universal function. Then if one wishes to combine the contributions of the two problems, the computational task is merely a matter of adding the two universal functions as indicated in Equation (9*b*).

A plot of the universal functions $q_T a/k\ (T_i - T_w)$ and q_{TS}/Sa has been prepared and is presented in Figure 2 as a function of $\xi = (x/a)/N_{Re}N_{Pr}$. It is seen that q_T attains an extremely high value at the duct entrance (theoretically infinite) and then decreases to zero at large downstream distances. On the other hand q_{TS} is zero at the entrance and increases monotonically with x, finally achieving the constant value Sa. If one defines an entrance length in terms of the distance required to arrive to within 5% of the fully developed condition, this would correspond to an $(x/a)/N_{Re}N_{Pr}$ of about 0.35 for q_{TS}. Such a definition for the entrance length is not appropriate to q_T, since its fully developed value is zero.

Consideration may now be given to the local heat transfer due to the combined action of temperature driving force $(T_i - T_w)$ and internal heat generation S. In evaluating Equation (9*b*) it may be noted that $Sa^2/k(T_i - T_w)$ may be either positive or negative. In practice it is highly likely that S will be positive, but $(T_i - T_w)$ may be either positive or negative. With this in mind illustrative heat transfer results have been evaluated from Equation (9*b*) for values of $Sa^2/k\ (T_i - T_w)$ ranging from −100 to

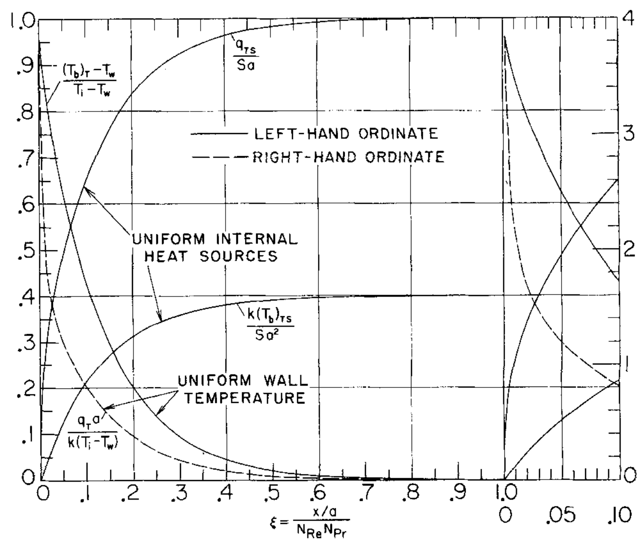

Fig. 2. Results for uniform internal heat source with zero wall and inlet temperature and for uniform wall temperature without internal heat sources.

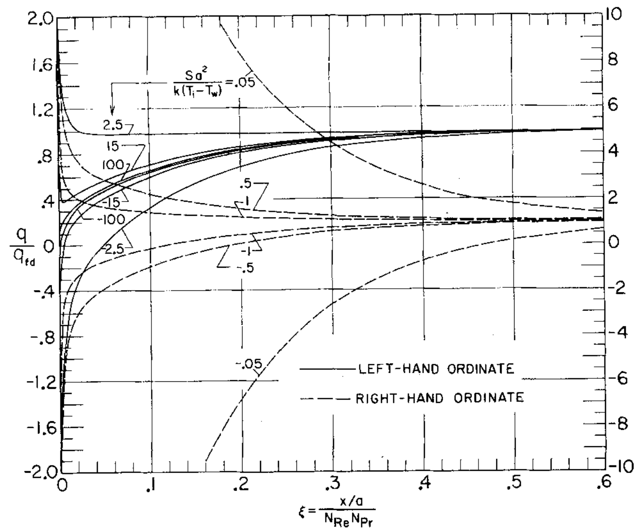

Fig. 3. Local heat flux results for internal heat generation with prescribed wall temperature.

+100. This information is given in Figure 3 as a function of the longitudinal position co-ordinate. The ordinate variable is the ratio of the local heat flux q at ξ to the fully developed heat flux $q_{fd} = Sa$.

An overall inspection of the figure reveals a variety of trends. In some cases q decreases with x, in others q increases with x, and in still others q at first decreases and then increases with x. To aid in explaining the results of this figure it may be recalled (for example from Figure 2) that at very small ξ the heat flux is essentially determined by the thermal driving force $(T_i - T_w)$, while for large ξ the heat flux is essentially determined by the internal heat generation. For convenience in discussion suppose that S is positive, so that q_{fd} is positive. Then a negative value of $Sa^2/k\ (T_i - T_w)$ implies $(T_i - T_w)$ is negative and consequently q_T is opposite in sign to q_{fd}. Therefore for this condition q/q_{fd} is negative when q_T dominates, that is at small values of ξ. With increasing x the contribution of q_T diminishes steadily, while that of q_{TS} becomes simultaneously more important. Therefore all curves characterized by negative values of $Sa^2/k\ (T_i - T_w)$ slope upward, finally achieving a value of unity for large ξ. The contribution of q_T persists for a lesser axial distance when $T_i - T_w$ is relatively small, that is when $Sa^2/k\ (T_i - T_w)$ is relatively large; for such cases the curves rise steeply.

When $Sa^2/k\ (T_i - T_w)$ is positive, both q_T and q_{TS} are positive. Because q_T dominates near the entrance, all curves approach plus infinity as x approaches zero. Additionally when $(T_i - T_w)$ is relatively small, that is large values of $Sa^2/k\ (T_i - T_w)$, the influence of q_T is confined to a very small range of x, with the consequence that q drops off very rapidly. A minimum may be reached before q_{TS} is large enough to contribute significantly to q. For smaller values of $Sa^2/k\ (T_i - T_w)$ the influence of q_T persists to ξ values large enough so that the minimum is not achieved.

The foregoing presentation of results has been concerned with the local heat transfer. Perhaps of equal interest is the overall rate of heat transfer Q from $x = 0$ to some location $x = x$:

$$Q = 2 \int_o^x q\, dx \qquad (10)$$

A convenient presentation of information for Q may be made in terms of the local bulk temperature $T_b(x)$, which is itself a quantity of some interest:

$$T_b = \left[\int_o^a Tudy \right] \Big/ \left[\int_o^a udy \right] \qquad (11)$$

Upon introduction of the foregoing expressions for q and T and integration, there is obtained after rearrangement

$$\frac{2Q}{k(T_i - T_w)N_{Re}N_{Pr}} = 1 + \frac{4\, Sa^2}{k(T_i - T_w)} \cdot \frac{x/a}{N_{Re}N_{Pr}} - \frac{T_b - T_w}{T_i - T_w} \qquad (12)$$

$$\frac{T_b - T_w}{T_i - T_w} = \left[\frac{(T_b)_T - T_w}{T_i - T_w} \right] + \frac{Sa^2}{k(T_i - T_w)} \left[(T_b)_{TS} \frac{k}{Sa^2} \right] \qquad (13)$$

in which

$$\frac{(T_b)_T - T_w}{T_i - T_w} = -\frac{3}{2} \Sigma\ (C_{n,T}/\beta_n^2)\ Y_n'(1)\ e^{-(8/3)\beta_n^2\xi} \qquad (13a)$$

$$\frac{(T_b)_{TS}\, k}{Sa^2} = \frac{2}{5} - \frac{3}{2} \Sigma\ (C_{n,TS}/\beta_n^2)\ Y_n'(1)\ e^{-(8/3)\beta_n^2\xi} \qquad (13b)$$

The bracketed quantities in Equation (13), which are written explicitly in Equations (13*a*) and (13*b*), have a definite physical meaning. The first represents the bulk temperature for the nongenerating fluid with entering temperature T_i and wall temperature T_w. The second represents the bulk temperature for the heat generating fluid with an entry and wall temperature equal to zero. Inspection of Equations (13*a*) and (13*b*) shows that each depends only on the position variable ξ and is independent of the thermal conditions of the problem. Consequently each can be evaluated once and for all. These universal functions are given in Figure 2. The $(T_b)_{TS}k/Sa^2$ curve rises steadily from its initial value of zero to an asymptote of 0.4 Sa^2/k for large ξ. The curve of $[(T_b)_T - T_w]/[T_i - T_w]$ decreases from an initial value of unity to an asymptote of zero as $(T_b)_T$ varies from T_i to T_w.

The heat transfer Q is calculable from Equation (12) as soon as the bulk temperature is available. This in turn may be obtained for any value of $Sa^2/k\ (T_i - T_w)$ from Equation (13) and Figure 2 by a simple additive operation. To illustrate the interplay between tht two contributions to

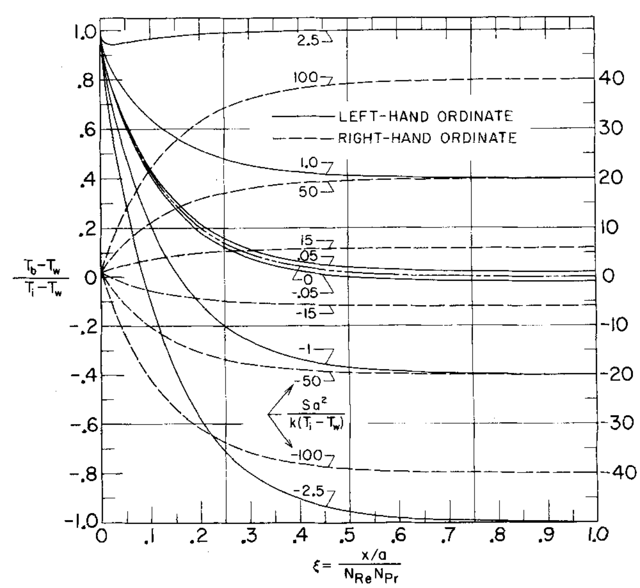

Fig. 4. Bulk temperature results for internal heat generation with prescribed wall temperature.

the bulk temperature, as well as to provide numerical data, Figure 4 has been prepared. This is a plot of $(T_b - T_w)/(T_i - T_w)$ as a function of the longitudinal position coordinate for parametric values of $Sa^2/k\ (T_i - T_w)$. As was also the case for Figure 2, one sees a variety of trends in Figure 4 depending upon whether $Sa^2/k\ (T_i - T_w)$ is negative or positive and also, when positive, on the specific magnitude. These trends occur for reasons similar to those delineated in connection with Figure 2; namely that the contributions of the nongenerating problem are dominant at small ξ, while the contributions of the problem with generation are dominant at large ξ. Further discussion would add little to what has been said in connection with Figure 2.

As a final note it should be pointed out that since the heat transfer processes with and without heat generation are independent, they can begin at different longitudinal positions without complicating the analysis. In other words the origin of the x coordinate for θ_T, q_T, and $(T_b)_T$ can be different from that for θ_{TS}, q_{TS}, and $(T_b)_{TS}$.

Transversely-Variable Internal Heat Generation

Consider the situation in which both wall temperature and internal heat generation are longitudinally uniform as before, but now the latter may vary arbitrarily across the section in a manner which is symmetric about the center line. The temperature T separates into T_T and T_{TS} as given by Equations (2a) and (2b). The T_T solution remains unchanged, as does q_T and $(T_b)_T$. The analysis for T_{TS} is modified without difficulty. First of all the heat source may be written as

$$S(\eta) = \overline{S}\varphi(\eta), \quad \overline{S} = \int_0^1 S d\eta \qquad (14)$$

and this is introduced into Equation (3). The solution for θ_{TS} follows from Equation (8) by replacing S by $\overline{S}$ and writing

$$\chi = \int_\eta^1 \left[\int_0^{\eta'} \varphi(\eta'')\, d\eta'' \right] d\eta' \qquad (15)$$

in lieu of $\frac{1}{2}(1-\eta^2)$. The η' and η'' are dummy variables. The expression for $C_{n,TS}$ follows as

$$C_{n,TS} = -\left[\frac{1}{\beta_n^2} \int_0^1 Y_n \varphi\, d\eta \right] \Bigg/ \left[\int_0^1 Y_n^2\, (1-\eta^2) d\eta \right] \qquad (15a)$$

It is easily verified that the foregoing equations reduce to (8) and (8a) when $\varphi = 1$.

The local heat flux q_{TS} due to the heat generation is most conveniently found by modifying the last term on the right of Equation (9a). It is only necessary to replace the S which multiplies the bracket by $\overline{S}$. The overall heat transfer Q is calculable from Equation (12) as before, with the modification that the term 2/5 in Equation (13b) is replaced by

$$3/2 \int_0^1 \chi\, (1-\eta^2)\, d\eta \qquad (16)$$

The $C_{n,TS}$ is to be evaluated from Equation (15a).

It is seen from the foregoing that the transverse variation offers no particular difficulties.

Longitudinal Variations of Heat Generation and Wall Temperature

Even with longitudinal variations the linearity of the energy equation permits subdivision of the temperature T into the sum $T_T + T_{TS}$. It is convenient to solve separately for each of these.

Considering first T_T (that is no internal heat generation) it is useful to rewrite the solution, Equation (6), for uniform T_w as

$$T_T(x, y) - T_i = (T_w - T_i)\ [1 - \Sigma\, C_{n,T}\, Y_n\, e^{-(8/3)\beta_n^2 \xi}] \qquad (6a)$$

Suppose that instead of a finite jump of wall temperature at $\xi = 0$ from T_i to T_w, there is an infinitesimal change from T_i to $(T_i + dT_w)$ applied at $\xi = \xi^*$. For this, Equation (6a) applies when $\xi \geqslant \xi^*$, provided that $(T_w - T_i)$ is replaced by dT_w and ξ by $(\xi - \xi^*)$. Any arbitrary continuous variation in $T_w(\xi)$ can be envisioned as being made up of a series of steps dT_w, and the total contribution of these to $T_T(x,y)$ is found by integration:

$$T_T(x,y) - T_i = \int_0^\xi [1 - \Sigma\, C_{n,T}\, Y_n\, e^{-(8/3)\beta_n^2(\xi-\xi^*)}]\ d\,[T_w(\xi^*) - T_i] \qquad (17)$$

In addition to a continuous variation of T_w there may be any number of finite step jumps at locations ξ_{j1}, ξ_{j2}, etc. At each one of these step jumps a term

$$[1 - \Sigma\, C_{n,T}\, Y_n\, e^{-(8/3)\beta_n^2(\xi-\xi_j)}]\ \Delta T_j \qquad (17a)$$

is added to the integral, in which ΔT_j is the magnitude of the jump. Equations (17) and (17a) may be rephrased into the following alternate and perhaps more convenient form

$$T_T - T_i = -\frac{\partial}{\partial \xi}\left\{ \Sigma\, C_{n,T}\, Y_n \int_0^\xi [T_w(\xi^*) - T_i]\ e^{-(8/3)\beta_n^2(\xi-\xi^*)}\, d\xi^* \right\} + [T_w(\xi) - T_i] \qquad (18)$$

It is to be noted that Equation (18) takes account of all step jumps, although they do not appear explicitly.

Expressions for the local heat flux q and bulk temperature T_b follow directly from Equation (18) as

$$\frac{q_T\, a}{k} = \frac{\partial}{\partial \xi}\left\{ \Sigma\, C_{n,T}\, Y_n'(1) \int_0^\xi [T_w(\xi^*) - T_i]\ e^{-(8/3)\beta_n^2(\xi-\xi^*)}\, d\xi^* \right\} \qquad (19)$$

$$(T_b)_T - T_i = -4\, \Sigma\, C_{n,T}\, Y_n'(1) \int_0^\xi [T_w(\xi^*) - T_i]\ e^{-(8/3)\beta_n^2(\xi-\xi^*)}\, d\xi^* \qquad (20)$$

Longitudinal variations of the internal heat generation can be analyzed in a manner similar to that described in the foregoing. The volume rate of heat generation S is assumed expressible as a product

$$S(x,y) = \overline{S}(\xi)\varphi(\eta), \quad \overline{S} = \int_0^1 S d\eta \qquad (21)$$

The first stage in the generalization of the preceeding results for longitudinally uniform S is to find the response to an infinitesimal step dS applied at $\xi = \xi^*$. This response is then integrated over all such steps which form the prescribed distribution $\overline{S}(\xi)$. Further manipulation of this result leads to

$$\frac{T_{TS}\, k}{a^2} = -\frac{8}{3} \Sigma\, C_{n,TS}\, \beta_n^2\, Y_n \int_0^\xi \overline{S}(\xi^*)\ e^{-(8/3)\beta_n^2(\xi-\xi^*)} d\xi^* \qquad (22)$$

Differentiation of Equation (22) with respect to y provides an expression for the local heat flux q:

$$q_{TS}/a = \frac{8}{3} \Sigma\, C_{n,TS}\, \beta_n^2\, Y_n'(1) \int_0^\xi \overline{S}(\xi^*) e^{-(8/3)\beta_n^2(\xi-\xi^*)} d\xi^* \qquad (23)$$

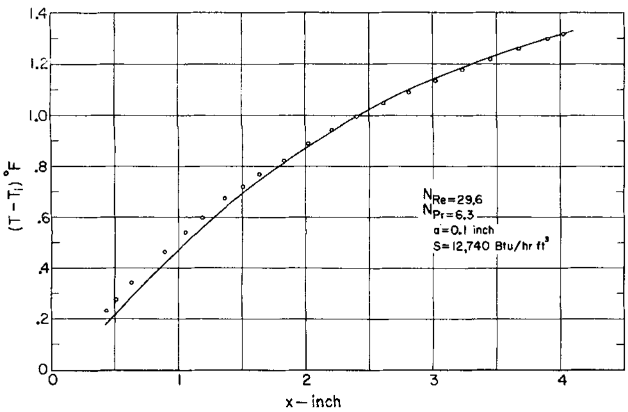

Fig. 5. Comparison of theoretical and experimental center-line temperatures.

Additionally integration of the solution for T_{TS} in accordance with Equation (11) gives the bulk temperature $(T_b)_{TS}$:

$$\frac{(T_b)_{TS}\,k}{a^2} = 4\,\Sigma\, C_{n,TS}\, Y_n'(1) \int_0^{\xi} \overline{S}(\xi^*)\, e^{-(8/3)\beta_n^2(\xi-\xi^*)}\, d\xi^* \qquad (24)$$

The separate results derived in the foregoing paragraphs may be combined by linear superposition

$$T = T_T + T_{TS},\ q = q_T + q_{TS},\ T_b = (T_b)_T + (T_b)_{TS} \qquad (25)$$

Finally the overall heat flux Q can be related to the bulk temperature as follows:

$$\frac{2Q}{k\, N_{Re} N_{Pr}} = \frac{4a^2}{k} \int_0^{\xi} \overline{S}(\xi)\, d\xi - (T_b - T_i) \qquad (26)$$

Thus arbitrary S and T_w are brought within the framework of the theory.

Experiments

The foregoing theory may be compared with some initial experimental results of research (9) currently in progress in the Heat Transfer Laboratory at the University of Minnesota. The apparatus consisted of a channel formed by two parallel plates separated by a distance of 0.2 in. A dilute electrolyte was pumped through the channel by natural circulation. An electric current flowing between the plates provided an essentially uniform heat generation in the fluid. The temperature distribution throughout the flow was determined by a Zehnder-Mach interferometer.

Figure 5 represents data for the longitudinal variation of the temperature at the center line. The test conditions are indicated in the figure. The wall temperature varied linearly with position and may be represented by

$$T_w - T_i = 0.0165x + 0.381, \quad (x = \text{in.},\quad T = {}^\circ\text{F.})$$

In addition to the data there is shown the prediction of analysis. The analytical curve is derived by superposing the T_{TS} from Equation (8) with the T_T from Equation (18), after the latter has been specialized for the aforementioned linearly varying wall temperature with step jump at $x = 0$. The agreement between theory and experiment is seen to be quite satisfactory. In the region near the entrance the data fell slightly higher than the theory; this is due to the effects of a simultaneously developing velocity profile.

INTERNAL HEAT GENERATION WITH PRESCRIBED WALL HEAT FLUX

The development for the case of prescribed surface heat flux may be carried out in a manner which parallels that already given for prescribed wall temperature. Therefore the details of the development may be omitted in favor of a concise presentation.

Uniform Heat Generation and Uniform Wall Heat Flux

The energy conservation principle continues to apply as written in Equation (2). The temperature T may be expressed as a sum $T_q + T_{qS}$, or in dimensionless form

$$\frac{T(x,y) - T_i}{q^*a/k} = \frac{T_q(x,y) - T_i}{q^*a/k} + \frac{T_{qS}(x,y)}{q^*a/k} = \theta_q + \theta_{qS} \qquad (27)$$

in which the symbol q^* corresponds to a positive heat flux into the fluid. The governing equations for θ_q and θ_{qS} become

$$\frac{1}{4}\frac{u}{\overline{u}}\frac{\partial \theta_q}{\partial \xi} = \frac{\partial^2 \theta_q}{\partial \eta^2},\quad \frac{1}{4}\frac{u}{\overline{u}}\frac{\partial \theta_{qS}}{\partial \xi} = \frac{\partial^2 \theta_{qS}}{\partial \eta^2} + \frac{Sa}{q^*} \qquad (28)$$

with boundary conditions

$$\text{at } \eta = \pm\, 1,\ \partial\theta_q/\partial\eta = \pm\, 1 \text{ and } \partial\theta_{qS}/\partial\eta = 0 \qquad (28a)$$

$$\text{at } \xi = 0,\ \theta_q = 0 \text{ and } \theta_{qS} = 0 \qquad (28b)$$

The T_q and T_{qS} problems have a definite physical meaning. The former is the case of uniform wall heat flux to a nongenerating fluid entering at temperature T_i. The latter is the case of a heat generating fluid with entering temperature of zero flowing in an insulated tube.

The solutions for θ_q and θ_{qS} are

$$T_q - T_i = \frac{q^*a}{k}\left\{ \frac{3}{4}\eta^2 - \frac{1}{8}\eta^4 - \frac{39}{280} + \frac{4x/a}{N_{Re}N_{Pr}} + \Sigma\, C_{n,q}\, Z_n\, e^{-(8/3)\gamma_n^2\xi} \right\} \qquad (29)$$

$$T_{qS} = \frac{Sa^2}{k}\left\{ \frac{1}{4}\eta^2 - \frac{1}{8}\eta^4 - \frac{11}{280} + \frac{4x/a}{N_{Re}N_{Pr}} + \Sigma\, C_{n,qS}\, Z_n\, e^{-(8/3)\gamma_n^2\xi} \right\} \qquad (30)$$

in which

$$C_{n,q} = -\frac{Z_n(1)}{\gamma_n^2 \int_0^1 Z_n^2(1-\eta^2)\, d\eta},$$

$$C_{n,qS} = -\frac{\int_0^1 Z_n\, d\eta}{\gamma_n^2 \int_0^1 Z_n^2(1-\eta^2)\, d\eta} \qquad (31)$$

The fully developed solutions for T_q and T_{qS} are found from Equations (29) and (30) by deleting the series. The bulk temperatures $(T_b)_q$ and $(T_b)_{qS}$ are readily obtained from an overall energy balance as

$$(T_b)_q - T_i = \frac{q^*a}{k}\frac{4x/a}{N_{Re}N_{Pr}},\quad (T_b)_{qS} = \frac{Sa^2}{k}\frac{4x/a}{N_{Re}N_{Pr}} \qquad (32)$$

TABLE 2. EIGENVALUES AND ASSOCIATED RESULTS,*

PRESCRIBED HEAT FLUX

n	γ_n	$Z_n(1)$	$C_{n,q}$	$C_{n,qS}$
1	4.2872	–1.2697	0.17503	0.046010
2	8.3037	1.4022	–0.051727	–0.0090443
3	12.3106	–1.4916	0.025053	0.0034072
4	16.3145	1.5601	–0.014924	–0.0016919
5	20.3171	–1.6161	0.0099692	0.00097989
6	24.3189	1.6638	–0.0071637	–0.00062610
7	28.3203	–1.7054	0.0054147	0.00042830
8	32.3214	1.7425	–0.0042475	–0.00030806
9	36.3223	–1.7760	0.0034280	0.00023026
10	40.3231	1.8066	–0.0028294	–0.00017742

* $Z_n(0) = 1$ for all n.

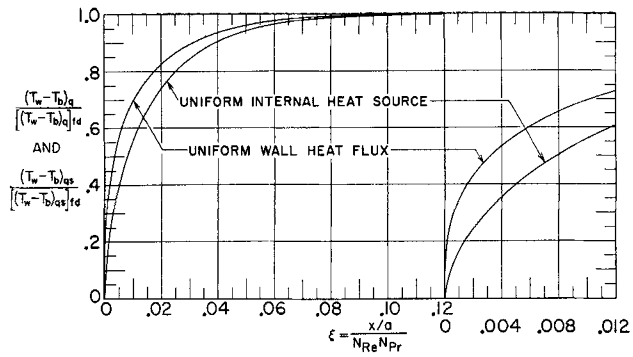

Fig. 6. Results for uniform internal heat source with adiabatic wall and for uniform wall heat flux without internal heat sources.

The γ_n^2 and Z_n appearing in Equations (29) and (30) are the eigenvalues and eigenfunctions of the mathematical system

$$d^2 Z_n/d\eta^2 + \gamma_n^2(1-\eta^2)Z_n = 0, \qquad d Z_n/d\eta = 0 \text{ at } \eta = 0, 1 \quad (33)$$

This differs from Equation (7) only in that the derivative rather than the function is zero at $\eta = 1$. The γ_n^2 and Z_n have been calculated by numerical means for $n = 1$ through 10. A listing of certain key values from these solutions is presented in Table 2. The information is of particular importance for calculating the longitudinal variation of tube wall temperature corresponding to a prescribed distribution of wall heat flux and internal heat generation. The values of γ_n^2 and $C_{n,q}$ for $n = 1$, 2, and 3 compare favorably with those of Cess (*10*).

Perhaps the quantity of greatest practical interest is the variation of the wall temperature as a function of position along the tube. A convenient presentation of this information may be made in terms of the wall-to-bulk temperature difference, which may readily be derived by evaluating Equations (29) and (30) at $\eta = 1$:

$$\frac{(T_w - T_b)_q}{[(T_w - T_b)_q]_{fd}} = 1 + \frac{35}{17}\Sigma C_{n,q} Z_n(1)\, e^{-(8/3)\gamma_n^2\xi}, \qquad [(T_w - T_b)_q]_{fd} = \frac{17}{35}\frac{q^* a}{k} \quad (34)$$

$$\frac{(T_w - T_b)_{qS}}{[(T_w - T_b)_{qS}]_{fd}} = 1 + \frac{35}{3}\Sigma C_{n,qS} Z_n(1)\, e^{-(8/3)\gamma_n^2\xi}, \qquad [(T_w - T_b)_{qS}]_{fd} = \frac{3}{35}\frac{Sa^2}{k} \quad (35)$$

From each of the foregoing equations it is evident that the ratio of the local wall-to-bulk temperature difference to the corresponding fully developed value is independent of the level of q or of S and depends only on the position variable ξ. These ratios have been evaluated from Equations (34) and (35) and are plotted in Figure 6, with details for the region of small ξ given in an inset at the right. From the figure it is seen that the wall-to-bulk temperature difference, beginning with a value zero, increases quite sharply in the neighborhood of the entrance. The increase of $|T_w - T_b|$ is more gradual at larger downstream distances, and finally, at still larger x, there is an asymptotic approach to the fully developed condition. It appears that the thermal development for the case of uniform wall heat flux is somewhat more rapid than that for the case of uniform heat sources, especially near the entrance. If the entrance length is defined in terms of a 5% approach to fully developed conditions, then this occurs at values of $(x/a)/N_{Re}N_{Pr} = 0.053$ and 0.045 respectively for prescribed S and prescribed q. For $N_{Re}N_{Pr} = 1{,}000$ this corresponds to a length equal to about twenty-five times the duct height.

The foregoing universal functions may be combined to provide results for the situation where q and S act simultaneously; thus

$$T_w - T_b = \frac{(T_w - T_b)_q}{[(T_w - T_b)_q]_{fd}}[(T_w - T_b)_q]_{fd} + \frac{(T_w - T_b)_{qS}}{[(T_w - T_b)_{qS}]_{fd}}[(T_w - T_b)_{qS}]_{fd} \quad (36)$$

The bulk temperature T_b for the combined process is found by summing $(T_b)_q$ and $(T_b)_{qS}$ from Equation (32). To illustrate the results Figures 7 and 8 have been prepared. To achieve a dimensionless presentation $(T_w - T_b)/(q^*a/k)$ is plotted (on the ordinate) as a function of the longitudinal position. The group Sa/q^* appears as a parameter, positive values of which are considered in Figure 7 and negative values in Figure 8. For convenience in discussion it may be supposed that S is positive (a heat source). Correspondingly a positive value of Sa/q^* would imply that q^* is positive; that is that heat is being transferred from the wall into the fluid. It follows that for this condition both the internal heat generation and wall heat transfer work together to produce values of $(T_w - T_b)$ which are larger than those for either process operating separately. This is why the curves in Figure 7 which are

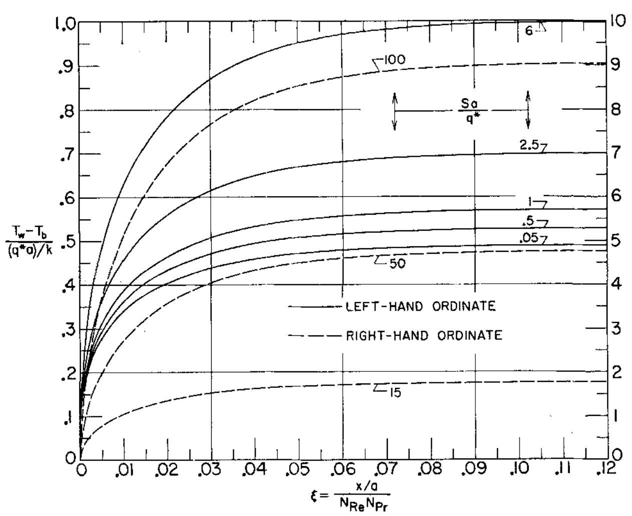

Fig. 7. Wall temperature results for internal heat generation with wall heat transfer, $Sa/q^* > 0$.

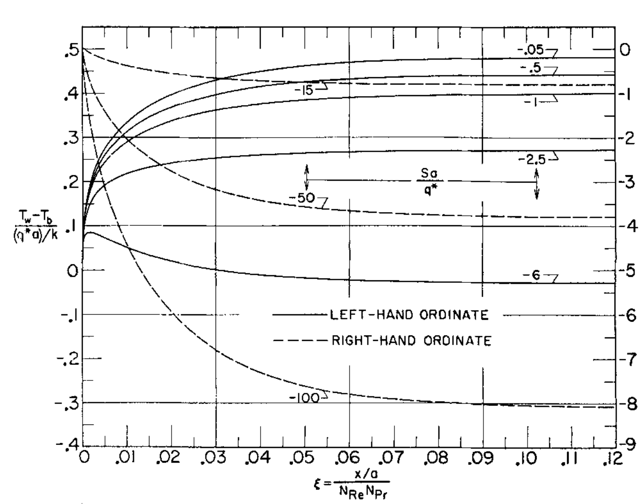

Fig. 8. Wall temperature results for internal heat generation with wall heat transfer, $Sa/q^* < 0$.

characterized by larger values of Sa/q^* lie higher than those which are characterized by low values of Sa/q^*. Additionally when both processes are re-enforcing one another, the monotonic increase of $(T_w - T_b)$ with ξ which was a characteristic of the separate processes, also applies. This may be verified by inspection of Figure 7, from which it may also be noted that the curves representing small values of Sa/q^* approach the fully developed state slightly more rapidly than those for larger Sa/q^*. This is consistent with the findings of Figure 6.

A negative value of Sa/q^* implies that q^* is negative (S positive). Consequently the internal heat generation and wall heat transfer are working in opposition. It is for this reason that a variety of trends are in evidence in Figure 8. For very small values of Sa/q^* wall heat transfer dominates, and the curves of $(T_w - T_b)/(q^*a/k)$ look very much like those for pure wall heat transfer. As $|Sa/q^*|$ takes on larger values, the internal heat generation becomes more important, and the curves are shifted downward. With further increases in Sa/q^* the effects of internal generation dominate, and the curves slope downward with increasing x. This is so except very near the entrance, where the wall heat transfer case continues to dominate because of its faster development (see Figure 6).

As was the case for prescribed wall temperature the linearity of the present situation implies that the onset of heating need not occur at the same position for the q and S problems.

Transversely-Variable Internal Heat Generation

It is once again convenient to express the cross-sectional variation of S as in Equation (14). The solution for T_q remains as given by Equation (29), but appropriate modifications must be made to generalize Equation (30) to apply to the case where S varies with y. The modifications are most easily incorporated by first defining

$$\Omega = \int_o^\eta \left[\int_o^{\eta'} \varphi(\eta'')d\eta'' \right] d\eta' \qquad (37a)$$

Then by substituting $\overline{S}$ for S and replacing the first three terms in the brace of Equation (30) by

$$\frac{3}{4}\eta^2 - \frac{1}{8}\eta^4 - \Omega + \frac{3}{2}\int_o^1 \Omega\,(1-\eta^2)d\eta - \frac{39}{280} \qquad (37b)$$

the generalization is accomplished. The series coefficients $C_{n,qS}$ are found from Equation (31), which is generalized by introducing the function $\varphi(\eta)$ into the numerator integrand. The wall-to-bulk temperature difference is found by evaluating the thus modified Equation (30) at $\eta = 1$.

There is an interesting and somewhat surprising relationship between the results for uniform internal heat generation and those for a parabolically transverse heat source. The latter distribution may be represented by

$$S = \overline{S}\left[\frac{A}{3+A} + \frac{3A}{3+A}\eta^2\right], A = \text{constant}$$

If the temperature solution corresponding to this transverse distribution of S is derived as outlined in the preceding paragraph, it is found that

$$\left[\frac{T-T_b}{\overline{S}a^2/k}\right]_{\text{para}} = \frac{3(A+1)}{(A+3)}\left[\frac{T-T_b}{\overline{S}a^2/k}\right]_{\text{uniform}}$$

In other words the results for the parabolic distribution of heat generation are a simple multiple of those for the case of uniform heat generation.

Longitudinal Variations of Heat Generation and Wall Heat Flux

The generalization of the foregoing results to the situation where longitudinal variations are present is accomplished by the superposition of infinitesimal steps in q and in S. The superposition method closely parallels that which has already been described for the case of prescribed surface temperature, and there is no need for repetition here. The heat source distribution corresponds to the product form of Equation (21). The final result for the temperature distribution corresponding to prescribed $q^*(\xi^*)$ and $\overline{S}(\xi^*)$ is

$$T - T_i = \frac{a}{k}\left\{ \int_o^\xi q^*(\xi^*) \left[4 - \frac{8}{3}\Sigma\, C_{n,q}\, Z_n\, \gamma_n^2\, e^{-(8/3)\gamma_n^2(\xi-\xi^*)} \right] d\xi^* \right\} + \frac{a^2}{k}\left\{ \int_o^\xi \overline{S}(\xi^*) \left[4 - \frac{8}{3}\Sigma\, C_{n,qS}\, Z_n\, \gamma_n^2\, e^{-(8/3)\gamma_n^2(\xi-\xi^*)} \right] d\xi^* \right\} \qquad (38)$$

and

$$T_b - T_i = \frac{4a}{k}\int_o^\xi q^*(\xi^*)d\xi^* + \frac{4a^2}{k}\int_o^\xi \overline{S}(\xi^*)d\xi^* \qquad (39)$$

The wall temperature variation is found by taking the Z_n in Equation (38) at $\eta = 1$.

ACKNOWLEDGMENT

The research reported herein was supported by the U. S. Atomic Energy Commission under contract AT(11-1)-659.

NOTATION

- a = half height of duct
- c_p = specific heat, constant pressure
- C_n = series coefficients
- k = thermal conductivity
- N_{Pr} = Prandtl number, $c_p\mu/k$
- Q = overall heat transfer rate from fluid to wall
- q = local heat flux rate from fluid to wall
- q^* = local heat flux from wall to fluid
- N_{Re} = Reynolds number, $4a\overline{u}/\nu$
- S = heat generation rate/volume
- $\overline{S}$ = cross-sectional average of S, Equation (14)
- T = temperature
- u = local longitudinal velocity
- $\overline{u}$ = average velocity
- x = longitudinal coordinate
- Y = eigenfunctions of Equation (7)
- y = transverse coordinate
- Z = eigenfunctions of Equation (33)

Greek Letters

- β = eigenvalues of Equation (7)
- γ = eigenvalues of Equation (33)
- η = dimensionless coordinate, y/a
- θ = dimensionless temperature, Equations (2b) and (27)
- μ = absolute viscosity
- ν = kinematic viscosity
- ρ = density
- ξ = dimensionless coordinate, $(x/a)/N_{Re}N_{Pr}$
- φ = transverse variation of S, Equation (14)
- χ = heat source function defined by Equation (15)

Subscripts

b = bulk
fd = fully developed
i = inlet
q = wall heat flux, no internal generation
qS = insulated wall, internal heat generation
T = prescribed wall temperature, no internal generation
TS = zero wall temperature, internal heat generation

LITERATURE CITED

1. Topper, L., *Chem. Eng. Sci.*, 5, 13-19 (1956).
2. Sparrow, E. M., and R. Siegel, *Nucl. Sci. Eng.*, 4, 239-254 (1958).
3. Inman, R. M., *Internat. J. Heat and Mass Transfer*, 5, 1053-1059 (1962).
4. Siegel, R., and E. M. Sparrow, *J. Heat Transfer*, C81, 280-290 (1959).
5. Poppendiek, H. F., and L. D. Palmer, Oak Ridge National Laboratory, *Rept. ORNL-1701* (1954).
6. Loeffler, A. L., Jr., *Nucl. Sci. Eng.*, 2, 547 (1957).
7. Jakob, Max, "Heat Transfer," Vol. 1, Wiley, New York (1949).
8. Brown, G. M., *Am. Inst. Chem. Engrs. Journal*, 6, 179-183 (1960).
9. Novotny, J. L., Research in progress, Mechanical Engineering Department, University of Minnesota, Minneapolis, Minnesota.
10. Cess, R. D., and E. C. Shaffer, *Appl. Sci. Res.*, A8, 339-347 (1959).

Manuscript received March 15, 1963; revision received July 8, 1963; paper accepted July 10, 1963.

Behavior of Non-Newtonian Fluids in the Entry Region of a Pipe

MORTON COLLINS and W. R. SCHOWALTER

Princeton University, Princeton, New Jersey

The current trend toward a more scientific approach to engineering design has brought about the need for fundamental information concerning the behavior of non-Newtonian fluids in motion. Such information can be obtained by solving the differential equations of motion for non-Newtonian fluids. Exact solutions to these equations are possible only for relatively simple geometries and constitutive equations (the equations relating the stress condition of a fluid to its velocity field). Many problems are inherent in obtaining solutions to the equation of motion. A review by Oldroyd (*10*) treats some of these problems.

Approximate solutions to the equation of motion have been of vital importance in the advancement of Newtonian fluid mechanics, and hence it seems likely that similar approximate solutions will be valuable in the study of non-Newtonian fluids in motion. Thus the use of boundary-layer theory for non-Newtonian systems has been discussed by Schowalter (*14*), and specific applications have been reported by Acrivos, et al. (*1*) and Collins and Schowalter (*5*). In the present paper principles of boundary-layer theory have been applied to determine the behavior of a non-Newtonian fluid in the entry region of a pipe. The results apply to laminar flow of viscous pseudoplastic fluids whose rheological behavior can be approximated by a power-law relation between shear stress and velocity gradient.

Earlier workers (*3, 15*) have used approximate forms of boundary-layer theory to estimate the entry length for axisymmetric pipe flow. The present analysis differs from these in that a more realistic treatment of the boundary layer is utilized. The results provide estimates of the pressure drop which occurs in the entry region, the length of pipe required to establish fully developed laminar flow, and the shape of velocity profiles in the entry region. The technique used is an extension of that previously described by the authors (*5*). It is believed that the results provide a better description of velocity profiles in the entry region than has previously been available. The results should be helpful to persons interpreting pressure loss and heat transfer data taken under conditions such that the shape of the velocity profile is affected by proximity of the pipe entrance.

Morton Collins is with Esso Research and Engineering Company, Linden, New Jersey.

THEORY

Development of the basic equations is analogous to the procedure previously employed for flow in a two-dimensional channel (*5*). Consequently only essential points will be treated here.

Consider a pipe of radius a and a cylindrical coordinate system with its origin at the entry. The x axis is on the pipe center line, and the r axis is normal to the center line. The fluid is assumed to enter the pipe at $x = 0$ with a flat velocity profile ($u = U_o$, $v = 0$). Near the entry boundary-layer techniques are applicable, while in the region approaching fully developed flow the velocity profile may be described in terms of perturbations to fully developed flow. Results from the two methods of solution are joined at an appropriate value of x.

The analysis applies to fluids which can be characterized by Bird's generalization of the power law, which assumes that any effect of the third invariant is of second order (*2*):

$$\mu_{\text{eff}} = K\left(\frac{1}{2} I_2\right)^{\frac{n-1}{2}} \tag{1}$$

For the axisymmetric flow under consideration the approximation